ADVANCED ENERGY MATERIALS

Supporting Information

for *Adv. Energy Mater.,* DOI: 10.1002/aenm.201802398

Conductive Cellulose Nanofiber Enabled Thick Electrode for Compact and Flexible Energy Storage Devices

*Yudi Kuang, Chaoji Chen, Glenn Pastel, Yiju Li, Jianwei Song, Ruiyu Mi, Weiqing Kong, Boyang Liu, Yingqi Jiang, Ken Yang, and Liangbing Hu**

Supporting Information

Conductive Cellulose Nanofiber Enabled Thick Electrode for Compact and Flexible Energy Storage Devices

Yudi Kuang[1(a)], Chaoji Chen[1(a)], Glenn Pastel[1(a)], Yiju Li[1], Jianwei Song[1], Ruiyu Mi[1], Weiqing Kong[1], Boyang Liu[1], Yingqi Jiang[2], Ken Yang[2], Liangbing Hu[1,*]

1. Department of Materials Science and Engineering, University of Maryland, College Park, Maryland, 20742
2. Analog Devices Incorporated, Wilmington, Massachusetts, 01887

[*] Email: binghu@umd.edu

[a] These authors contributed equally to this work.

Figure S1. Photographs showing the preparation of the negatively charged CNF suspension. The micro-size cellulose pulp was pretreated by a 2,2,6,6-tetramethylpiperidine-1-oxyl (TEMPO) oxidization process, which selectively oxidized the C6-hydroxyl groups of the cellulose molecular chain to carboxyl groups, leading to a strong negatively charged surface of the cellulose fibers. Negatively charged CNF was then obtained by disintegrating the micro-size cellulose fiber down to the nanoscale via a probe sonication process for 1h. The clear and transparent appearance of the resultant solution indicating a good dispersion of the nano-size cellulose fibrils.

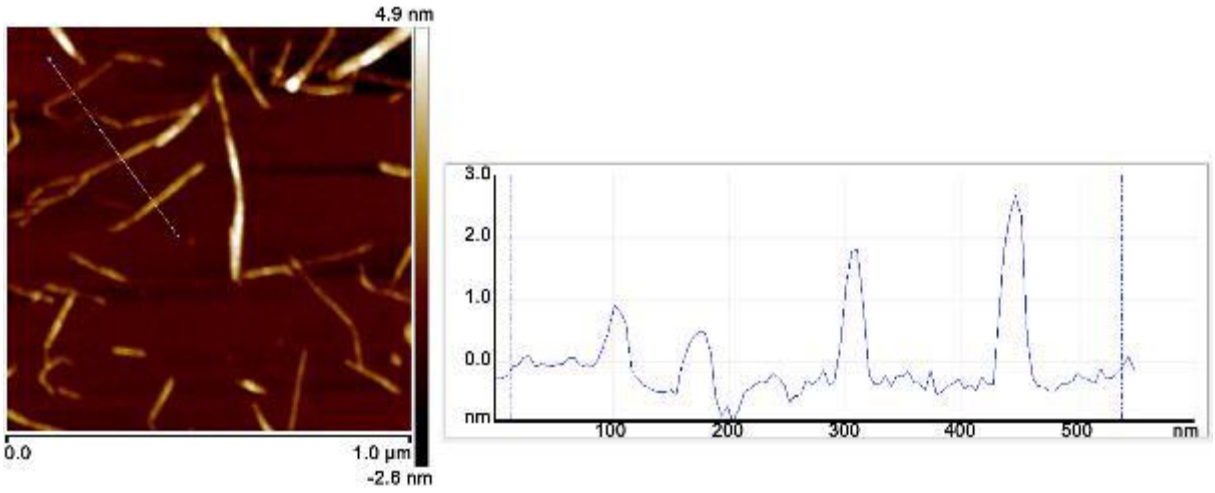

Figure S2. AFM image showing the morphology of the resultant cellulose nanofiber. To the right is the corresponding height plot of the cutting line in the AFM image, showing that the diameter of the cellulose nanofiber is approximately 1~3 nm.

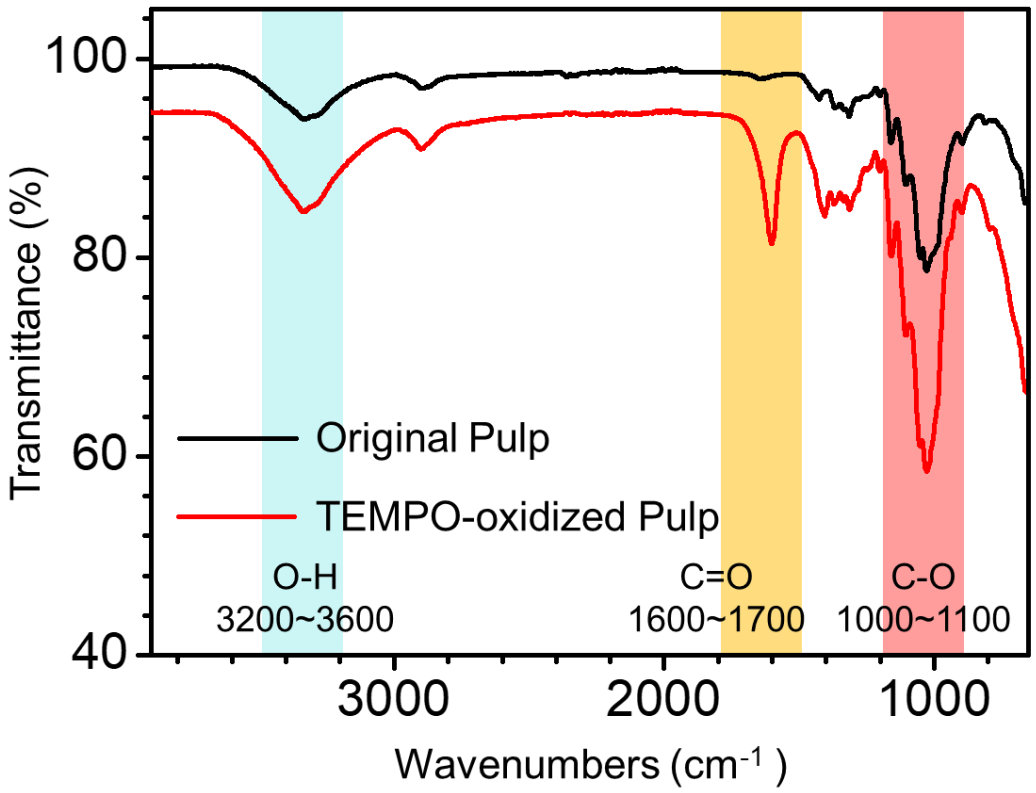

Figure S3. FI-IR plot of the cellulose pulp before and after TEMPO-Oxidization. The peaks around 3400 cm^{-1}, 1650 cm^{-1}, and 1030 cm^{-1} are represented by the O-H, C=O, and C-O stretch vibration absorption, respectively. The enhanced C=O and C-O peaks of TEMPO-oxidized pulp indicate the C6-hydroxyl groups have successfully oxidized to carboxyl groups.

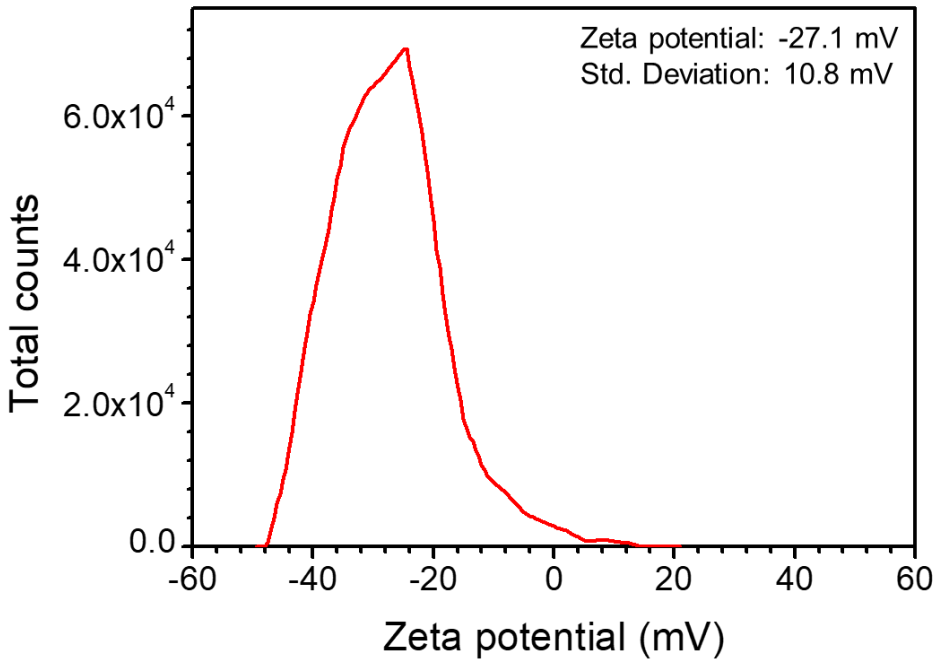

Figure S4. Zeta potential distribution of the TEMPO-oxidized cellulose pulp (0.1 wt% in water).

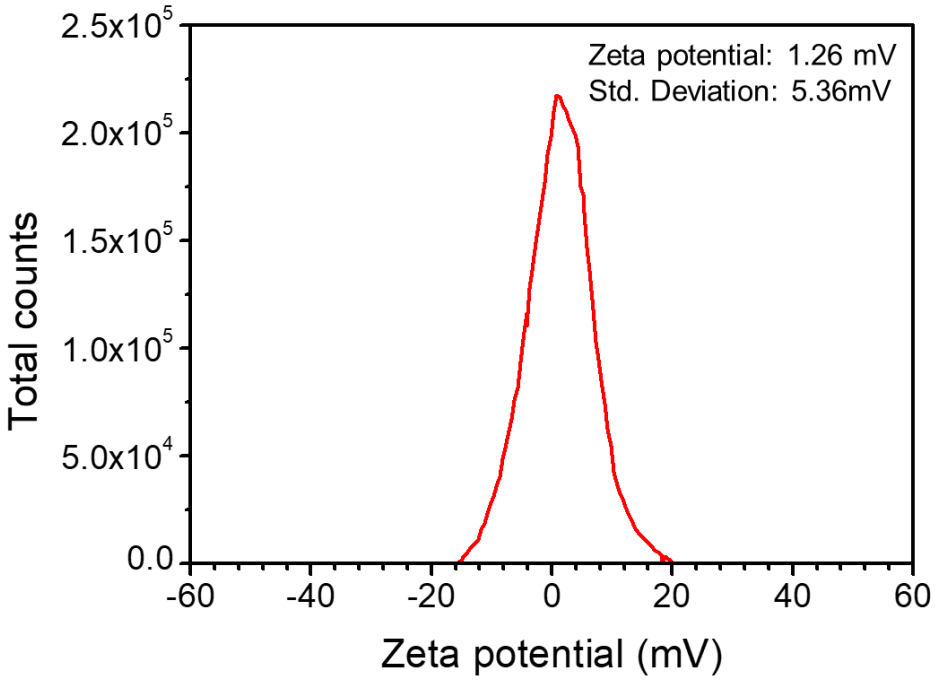

Figure S5. Zeta potential distribution of the CB suspension (0.1wt% in ethanol).

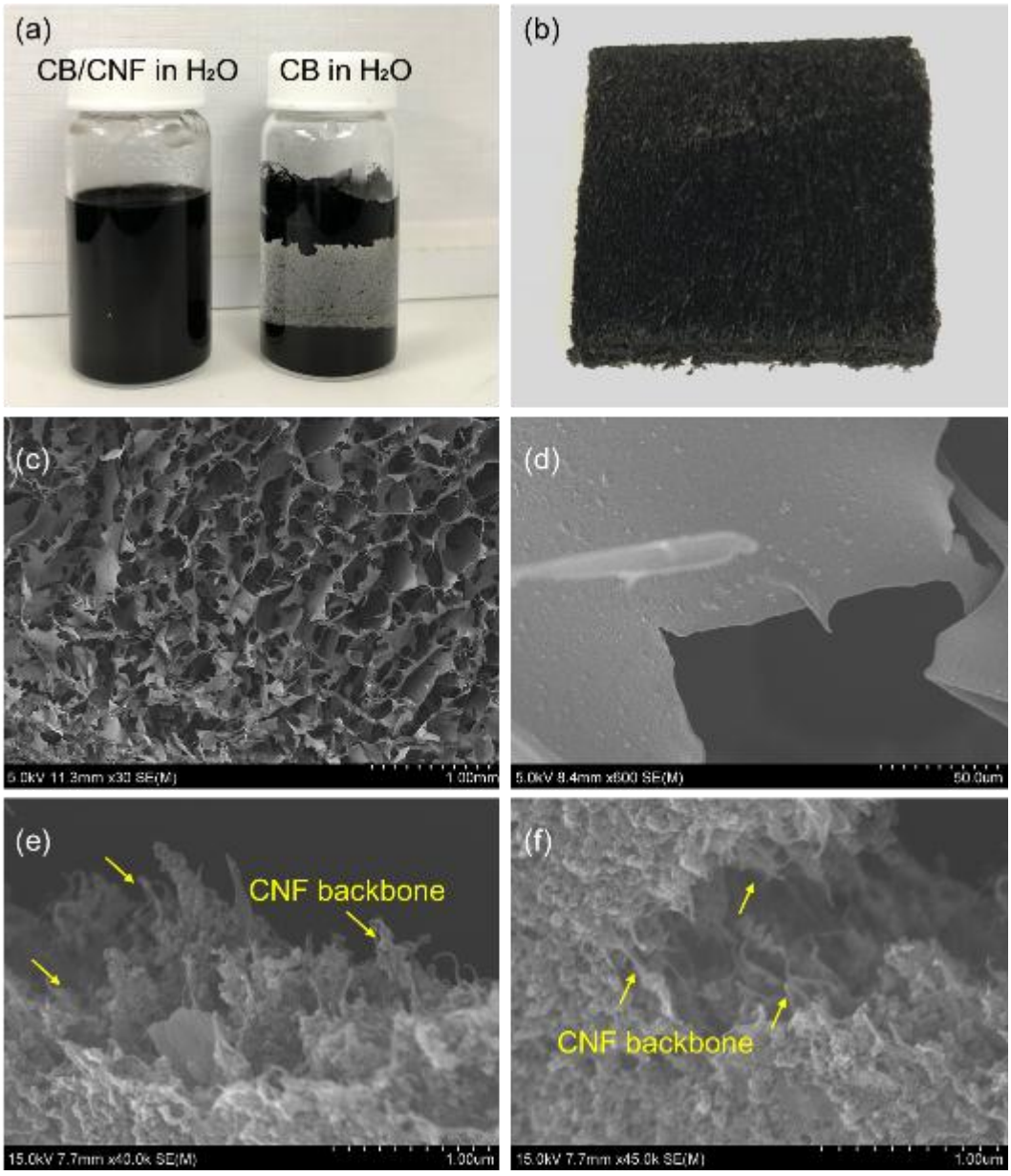

Figure S6. (a) Dispersibility of the CB in CNF suspension and aqueous solution. (b) Photograph of the conductive CNF/CB aerogel. (c-f) Morphological characterization of the conductive CNF/CB network.

Table S1. Summary of the nanopaper electrodes with different CNF-to-CB ratio.

Sample name	Composition	Resistance	Areal capacity (mAh cm^{-2})	Over potential (V)
CNF6*	80LFP : 6CNF : 14CB	-	-	-
CNF10	80LFP : 10CNF : 10CB	51.4 Ω	3.36	0.0786
CNF14	80LFP : 14CNF : 6CB	0.62 kΩ	2.58	0.2344
CNF18	80LFP : 18CNF : 2CB	39.22 MΩ	0.71	0.8340

*The strength of the sample is not strong enough to make a free-standing electrode.

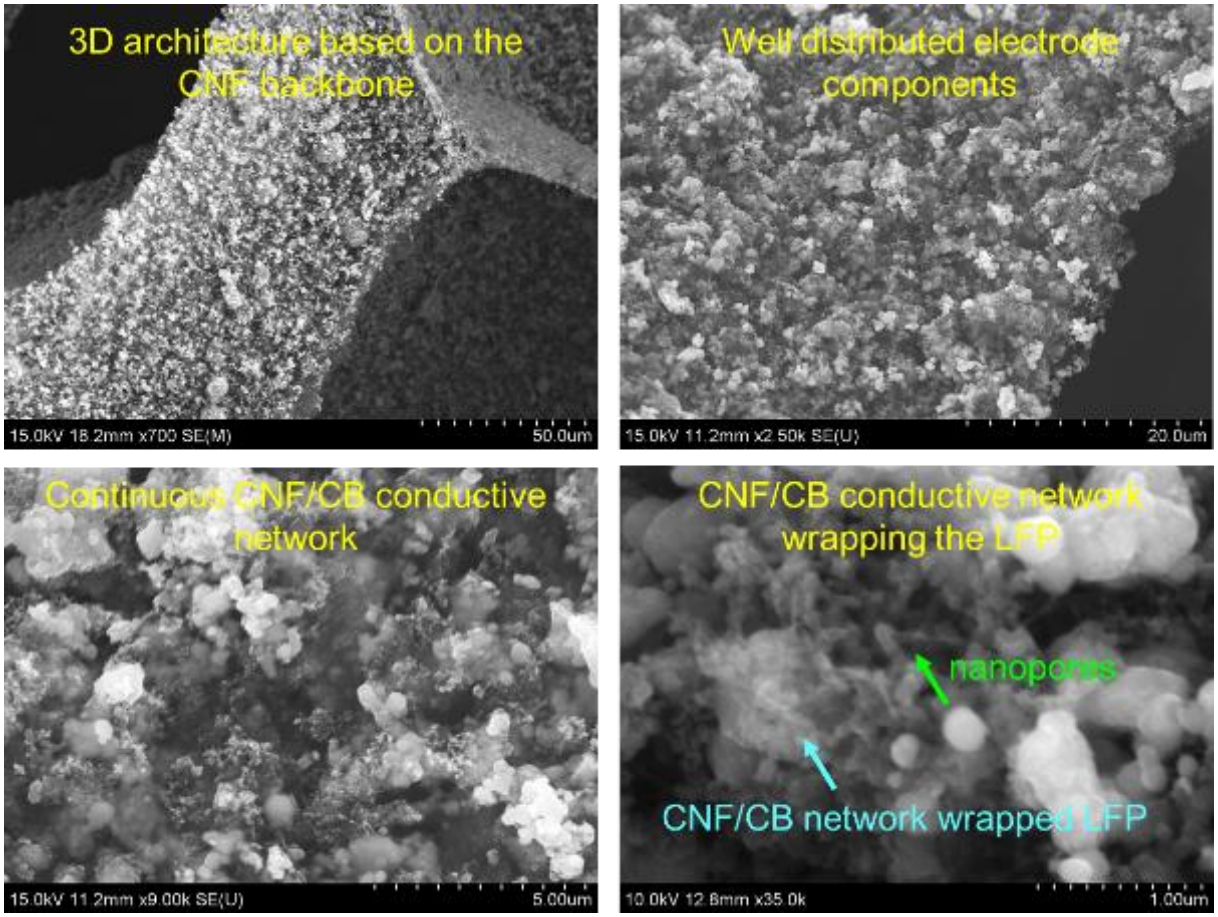

Figure S7. SEM image showing the hierarchical structure of the conductive CNF based electrode. Uniform distribution of CB and LFP particles are observed based on the interconnected CNF backbone.

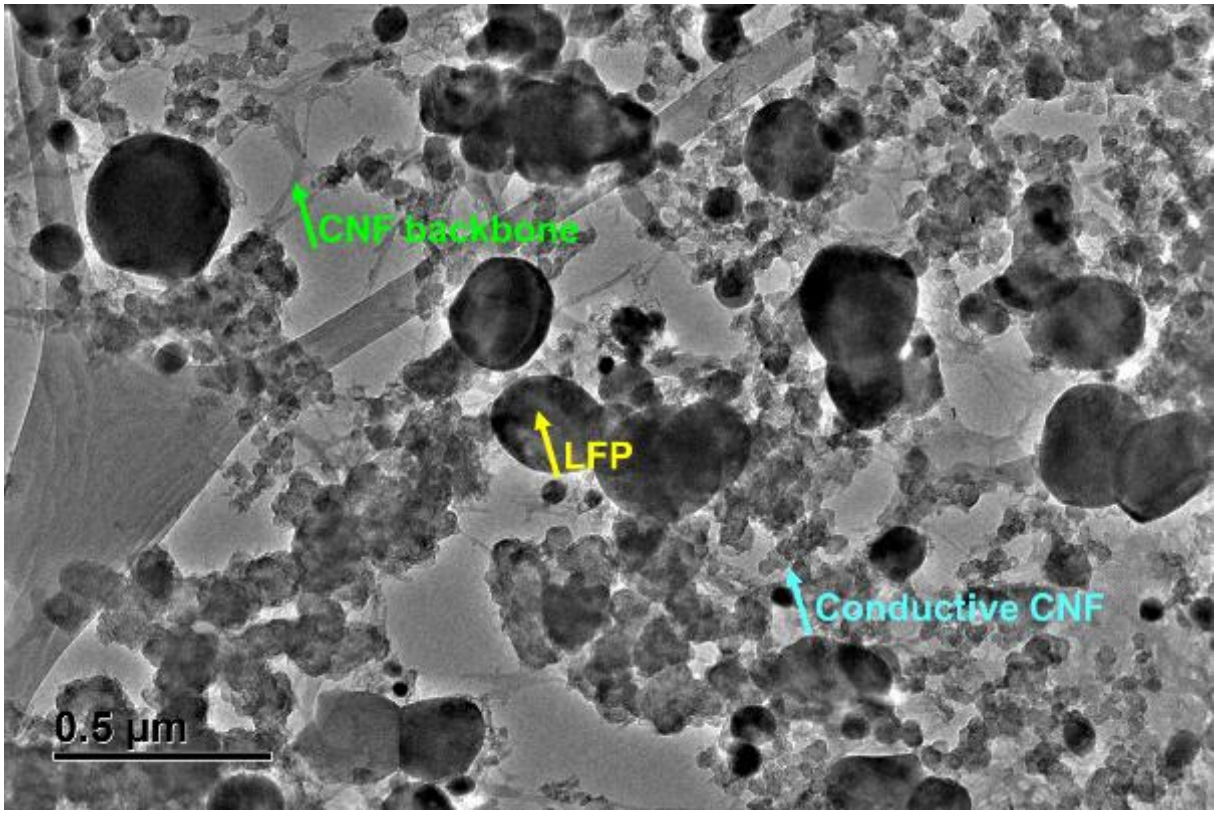

Figure S8. TEM images illustrating the uniform distribution of electrode components (CB, LFP, and CNF) and continuous conductive CNF network in the nanopaper electrode.

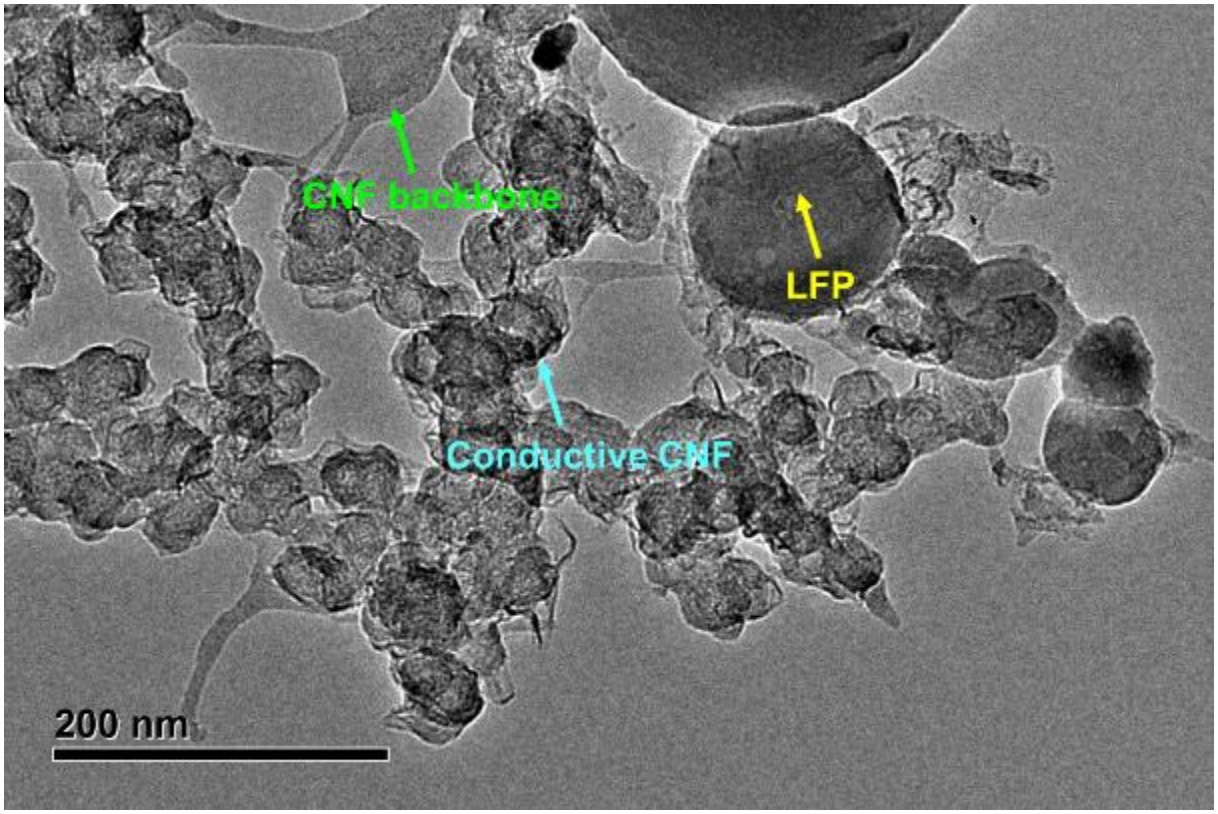

Figure S9. High-magnification TEM image showing that the CB nanoparticles are distributed along the CNF network, forming a continuous conductive pathway.

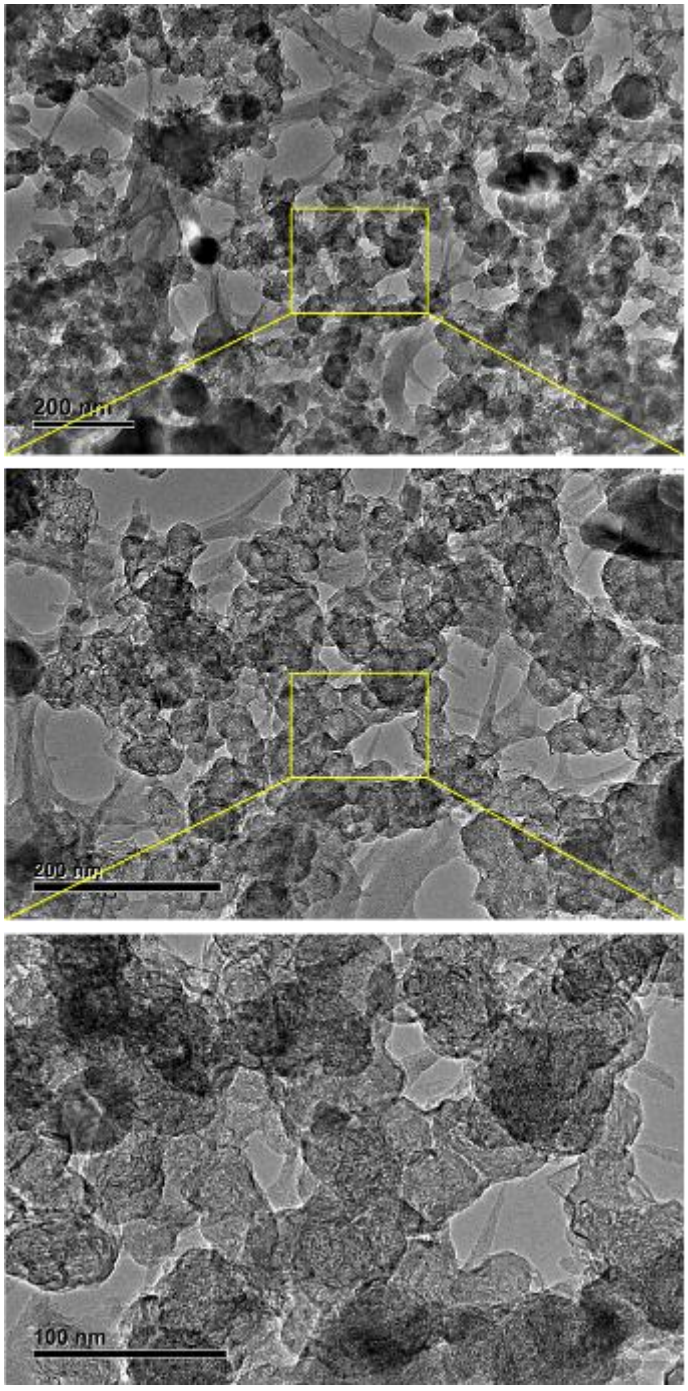

Figure S10. High resolution transmission electron microscopy (HRTEM) images of the conductive CB-CNF network. HRTEM illustrates that the CB nanoparticles in the nanopaper electrode are well attached on the CNF network and connected with each other, which forms a continuous conductive network. No isolated CB particles or aggregations are observed, suggesting a good interaction between the CNFs and CBs.

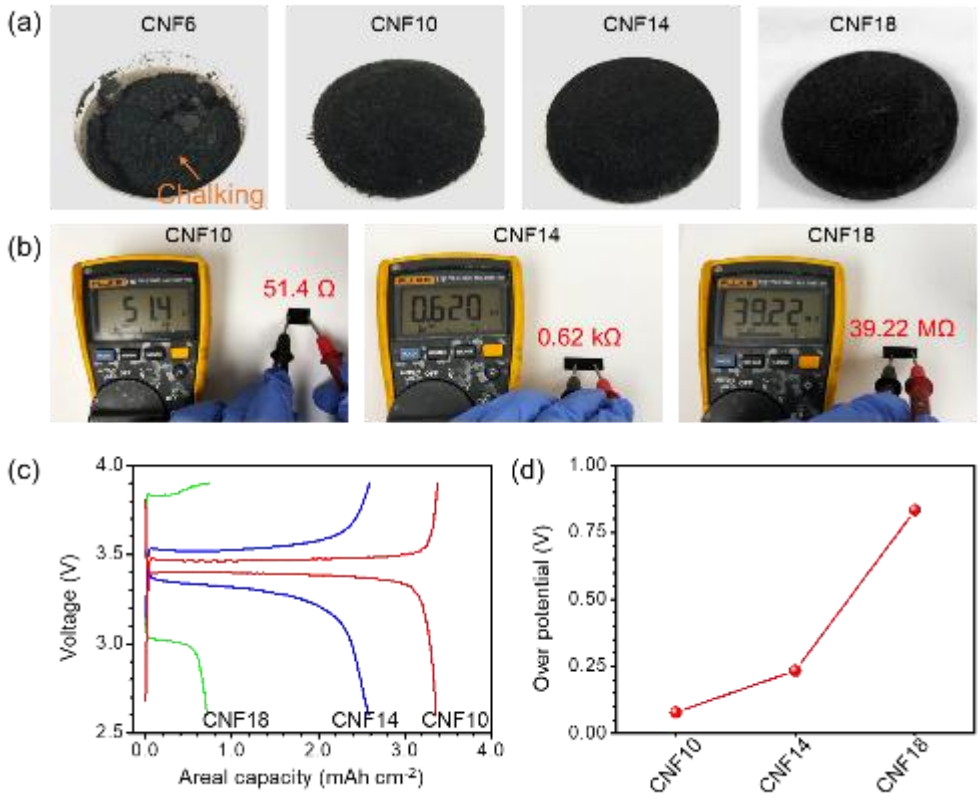

Figure S11. (a) Photographs of the LFP-CNF-CB aerogel electrodes with various CNF-to-CB ratios. (b) Conductivity measurements of the aerogel electrodes after pressing. (c) Charge-discharge profiles of the nanopaper electrodes with varying CNF-CB ratios at 0.5 mA cm^{-2}. (d) Overpotential of the corresponding nanopaper electrodes. The mass loading of the electroactive materials is 20 mg cm^{-2}.

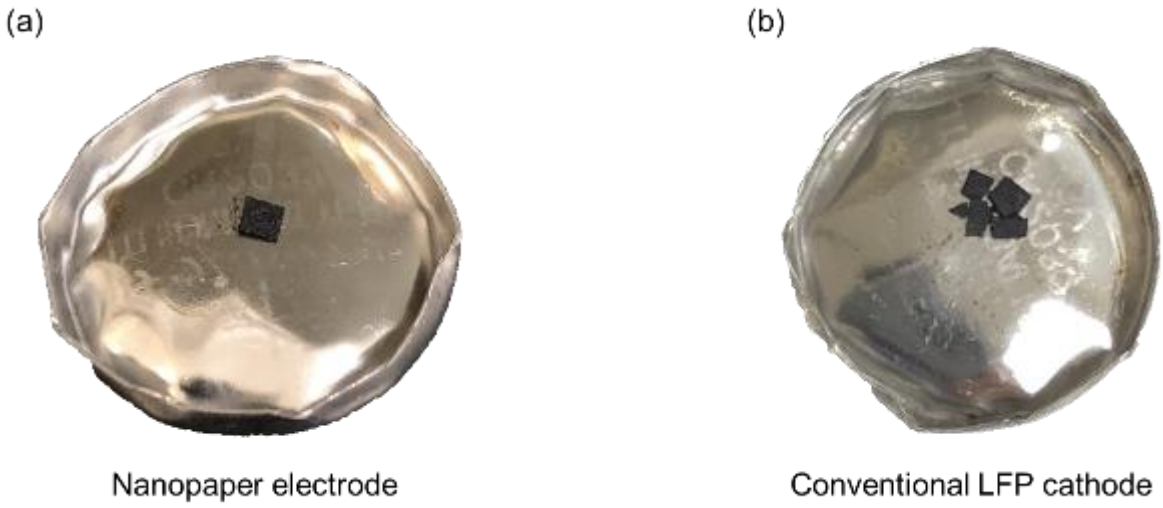

Figure S12. Photographs showing the mechanical stability of the electrodes (40 mg cm^{-2}) after cycling at current density of 2 mA cm^{-2} for 150 cycles. (a) The nanopaper electrode has maintained the original shape after cycling, while (b) the conventional thick LFP cathode has broken into pieces under the pressure of coin cell assembly.

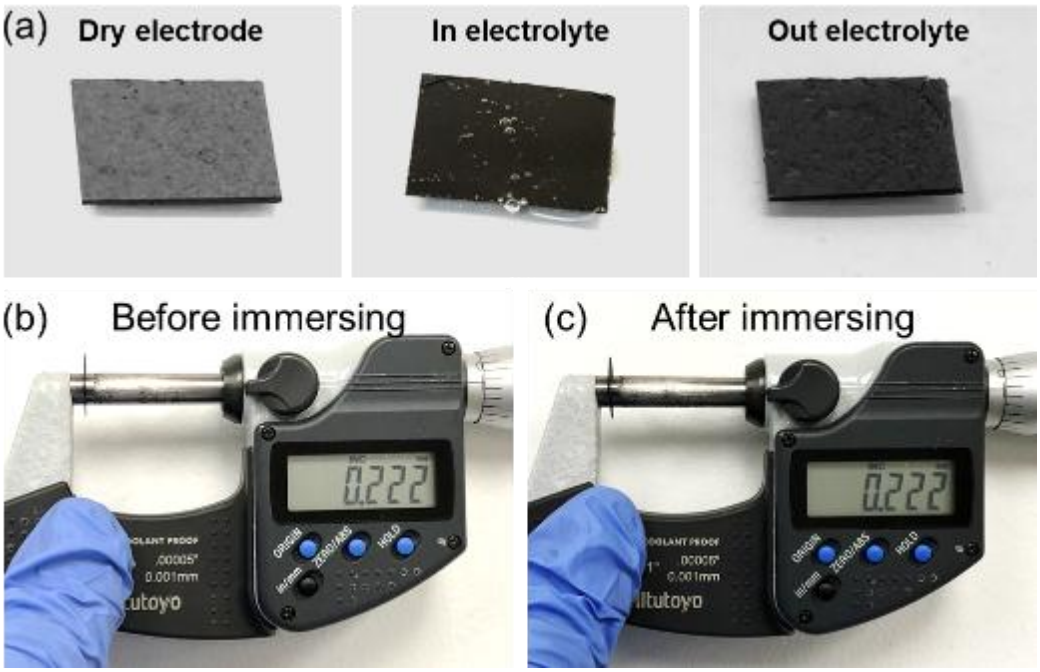

Figure S13. Photographs illustrating the structural durability of the nanopaper electrode after immersing in electrolyte. (a) Appearance of the nanopaper electrode in a dry-state, immersed in electrolyte, taken out of the electrolyte after sufficient immersion. (b) No thickness change was observed after sufficient immersion in electrolyte.

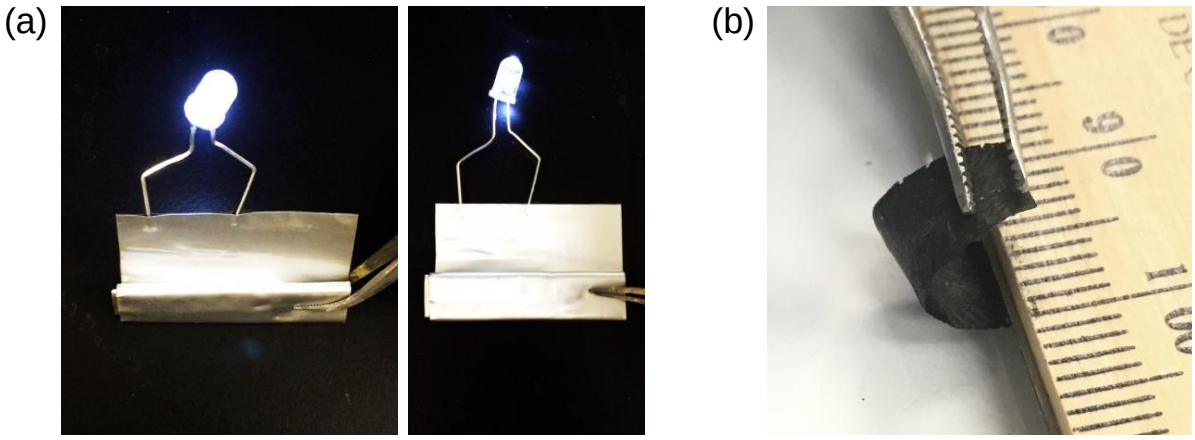

Figure S14. (a) Folded pouch cell with the compact nanopaper electrode as the cathode and thin lithium foil as the anode. (b) Photograph showing the flexibility of the nanopaper electrode with a mass loading of 20 mg cm^{-2}.

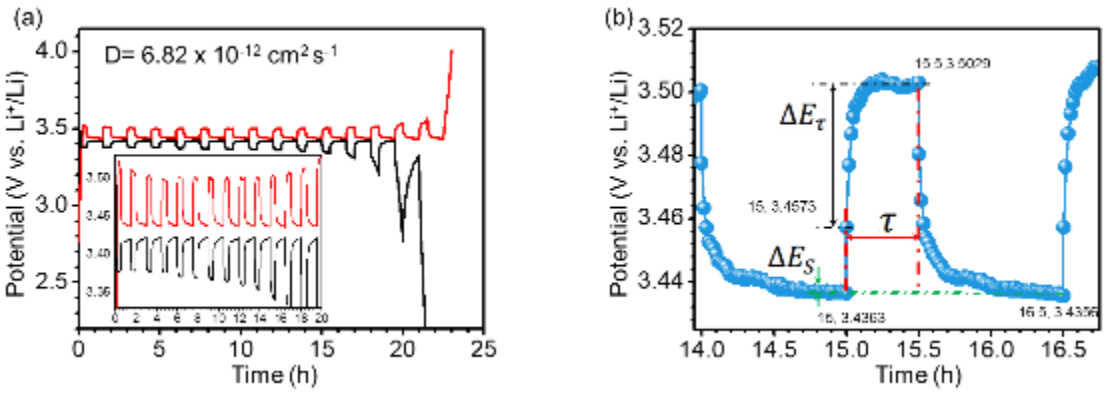

Figure S15. Kinetic analysis of conventional LFP cathode. (a) GITT plot of the conventional LFP cathode. (b) GITT profile showing the 11th delithiation process of the conventional LFP cathode.

The equation to determine diffusion coefficients of the nanopaper electrode and conventional LFP cathode is:

$$D = \frac{4}{\pi\Delta\tau}\left(\frac{m_B V_M}{M_B S}\right)^2\left(\frac{\Delta E_S}{\Delta E_\tau}\right)^2$$

Where m_B and M_B indicate the mass and molar mass of the electroactive material, respectively. V_m is assigned to the molar volume of the electrode materials, S is the geometric area of the electrode. Here, M_B = 157.76 g mol^{-1}, V_M = 46 cm^3 mol^{-1}, m_B/S represents the areal mass loading of the electrode. Other parameters in the equation such as $\Delta\tau$, ΔE_S and ΔE_τ are displaced in Figure 5 and Figure S10 for compact nanopaper electrode and conventional LFP cathode.

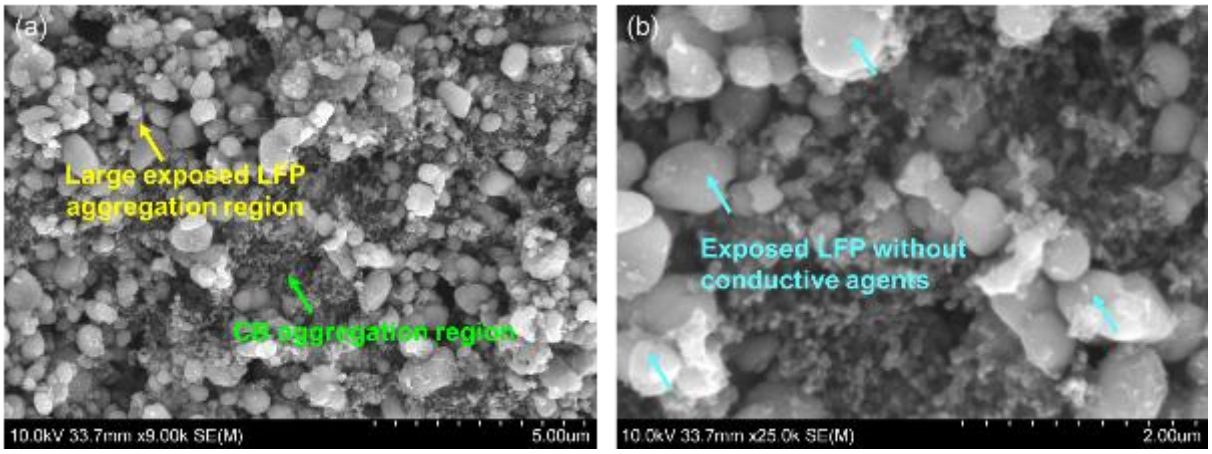

Figure S16. SEM images showing the microstructure of the conventional LFP:CB:PVDF electrode with a ratio of 8:1:1. (a) CB nanoparticles turn to aggregate in the electrode due to their large specific area, leading to a nonuniform conductive network and large area of (b) exposed LFP particles.

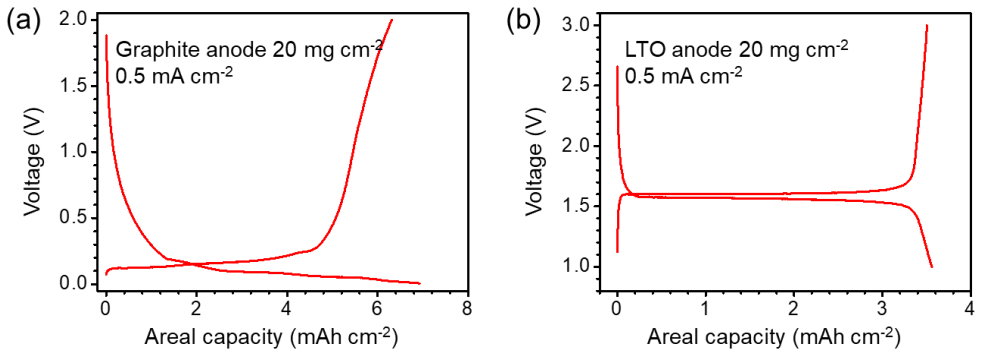

Figure S17. Charge-discharge profiles of (a) the graphite nanopaper electrodes and (b) LTO nanopaper electrodes at 0.5 mA cm^{-2}. The mass loading of the electrode active materials is 20 mg cm^{-2}.